Optimizing Ultrasonic Forgings Inspection by combining Pulse-Compression technique and multi-frequency AVG analysis

M.K. Rizwan[1], L. Senni[1], S. Laureti[1], P. Burrascano[1], M. Ricci[2]
1 University of Perugia, Dept. of Engineering, Italy,
{muhammadkhalid.rizwan, luca.senni, stefano.laureti, pietro.burrascano}@unipg.it
2 University of Calabria, Dept. DIMES, Italy, m.ricci@dimes.unical.it

Abstract

Ultrasonic pulse-echo NDT combined with AVG – Distance Gain Size - analysis is still the main method used for the inspection of forgings such as shafts or discs. Such method allows the inspection to be carried out in most of the cases assuring the necessary sensitivity and defect detection capability. However, when samples characterized by large dimensions and/or high attenuation are considered, the maximum Signal-to-Noise Ratio level achievable with standard pulse-echo presents major limitations due to the contextual action of the geometrical aperture of the ultrasound beam and of the physical attenuation of the beam energy during the propagation. To face this issue, the application of the pulse compression technique to the ultrasonic inspection of forgings was proposed by some of the present authors in combination with the use of broadband ultrasonic transducers and broadband chirp excitation signal. Here we extend the method by applying to pulse-compression data a specific multi-frequency AVG analysis that allows the evaluation of the sample as various samples simultaneously. The results of this analysis are compared with those of the standard single-frequency AVG method on a forging having known defects. It is show that the AVG analysis works fine with pulse-compression data collected by using a separated transmitter and receiver transducer. Moreover, narrowband analysis and broadband analysis provide almost identical results, but the latter allows the inspection frequency to be optimized with the use of a single transducer pair.

1. Introduction

Ultrasonic NDT is the only technique that allows the inspection of the entire volume of large forgings.
Pulse-echo (PuE) is the more diffused method for which all the Standards and evaluation procedures have been developed. Among these, the analysis based on the Distance Gain Size diagrams, henceforth called with the German acronym AVG, is the standard method allowing the sizing of defects in large structures where the use of DAC curve is not feasible [1-3]. Various probes at difference incidence angles and with different central frequencies are used to guarantee the inspection of the whole sample's volume with an adequate sensitivity for each possible type of defect present in it. AVG analysis with PuE is effective in most of the situations nevertheless two main critical points emerge: 1) the need to automatize the inspection as much as possible makes not convenient the use of many different probes; 2) in presence of high attenuation and-or large dimensions of the forgings, PuE could not guarantee an adequate SNR and sensitivity. To face the former point, phased-array probes have been introduced making

the automatic inspection easier: a single phased-array probe can replace several standard probes and moreover, being possible to vary the focusing of the ultrasonic beam, the sensitivity can be increased where needed to address also the latter issue. Anyway, this is not enough in some critical applications requiring a high sensitivity even with very weak signals or high noise.

Recently we proposed to exploit pulse-compression (PuC) technique in combination with the use of two separate transducers, one transmitter -Tx- and one receiver -Rx-, and chirp signals to increase the SNR of the measurement and then to increase the defect detection sensitivity [4]. In the present work, the method is improved by developing a numerical simulation tool for calculating AVG curves for an arbitrary Tx-Rx configuration working with both single-element and phased-array probes. The resulting AVG diagrams are used to evaluate the size of known flat bottom hole defects realized on a steel forging. Two different AVG analysis procedures are implemented and compared: one makes use of a narrowband chirp signal and of a single-frequency AVG analysis, the other makes use of a broadband chirp signal and of a simultaneous multi-frequency AVG analysis. The paper is organized as follows: in Section 2 the basic theory of PuC is summarized; in Section 3 the multi-frequency AVG analysis is introduced; in Section 4 are reported experimental results and a comparison between single-frequency and multi-frequency AVG analysis. In Section 5 some conclusions and perspectives are drawn.

2. Pulse compression basic theory

Flaw detection through ultrasonic inspection consists of measuring the impulse response $h(t)$ of the sample under test with respect to a mechanical wave excitation. In standard PuE method, the impulse response $h(t)$ of the system under inspection is estimated by exciting the sample with a short pulse $\tilde{\delta}(t)$ and then recording the system response $\tilde{h}(t) = \tilde{\delta}(t) * h(t)$, where $*$ is the convolution operator. If $\tilde{\delta}(t)$ is short enough to cover uniformly the whole bandwidth of the transducers, the approximation can be considered very close to the true expected signals. On the contrary, in a PuC measurement scheme an estimate $\hat{h}(t)$ of $h(t)$ is retrieved by: (I) exciting the system with a coded signal $s(t)$; (II) measuring the output of the coded excitation $y(t) = s(t) * h(t)$; (III) applying to the output the so-called matched filter $\psi(t)$ [5]. At the end of the procedure we have:

$$\hat{h}(t) = \psi(t) * y(t) = \underbrace{\psi(t) * s(t)}_{\hat{\delta}(t)} * h(t) = \hat{\delta}(t) * h(t) \approx h(t) \qquad (1)$$

where the "pulse compression condition" $\psi(t) * s(t) = \hat{\delta}(t) \approx \delta(t)$ has been exploited. As in most of the applications, in the present paper the matched filter is defined as the time-reversed replica of $s(t)$, $\psi(t) = s(-t)$, so that $\hat{\delta}(t)$ turns out to be the autocorrelation function of $s(t)$. The PuC condition can be therefore assured by every waveform having a δ-like autocorrelation function; a huge literature is available on this topic (see for example [4,6-8]). In NDT applications, and in particular in the case of ultrasonic inspection, the most used waveform is the Linear Chirp (LC) that is the signal employed also for the present application.

LC is described by the expression [9]:

$$s(t) = A(t)sin\big(\Phi(t)\big) = A(t)sin\left(2\pi\left(f_1 t + \frac{f_2 - f_1}{2T}t^2\right)\right) \quad (2)$$

where T is the duration of the chirp signal, f_1 the start frequency, f_2 the stop frequency and $B = f_2 - f_1$ is the chirp bandwidth. $A(t)$ is a time-windowing function that modulates the amplitude of the chirp and $\Phi(t) = 2\pi\left(f_1 t + \frac{f_2 - f_1}{2T}t^2\right)$ is the chirp phase function that determines the instantaneous frequency of the signal accordingly with $f_{ist}(t) = {\Phi'(t)}/{2\pi}$. $A(t)$ it is used to reduce sidelobes of $\hat{\delta}(t)$ and in the present work the Tukey-Elliptical window it is used [10]. Other important properties of LC are a constant envelope and an almost flat power spectrum in the spanned frequency range $f \in [f_1, f_2]$. Experimentally, while PuE requires only one transducer that acts both as Tx and Rx, PuC based schemes usually employ two distinct Tx and Rx transducers to allow the excitation signal duration to be extended arbitrary. The increased complexity of the resultant procedure is justified by the benefits it can provide in terms of resolution and SNR enhancement. Indeed, by using two distinct transducers, the excitation signal can be as long as the typical inspection time (few milliseconds for steel forgings) and therefore thousands of times longer than typical pulses used in PuE, which duration is inversely proportional to the transducer bandwidth. This allows more energy to be delivered to the system, increasing the SNR. Moreover, it was found that PuC is optimal to reduce noise, both environmental and due to the quantization step introduced by the ADC [11,12].

Figure 1 summarizes the present PuC procedure adopted.

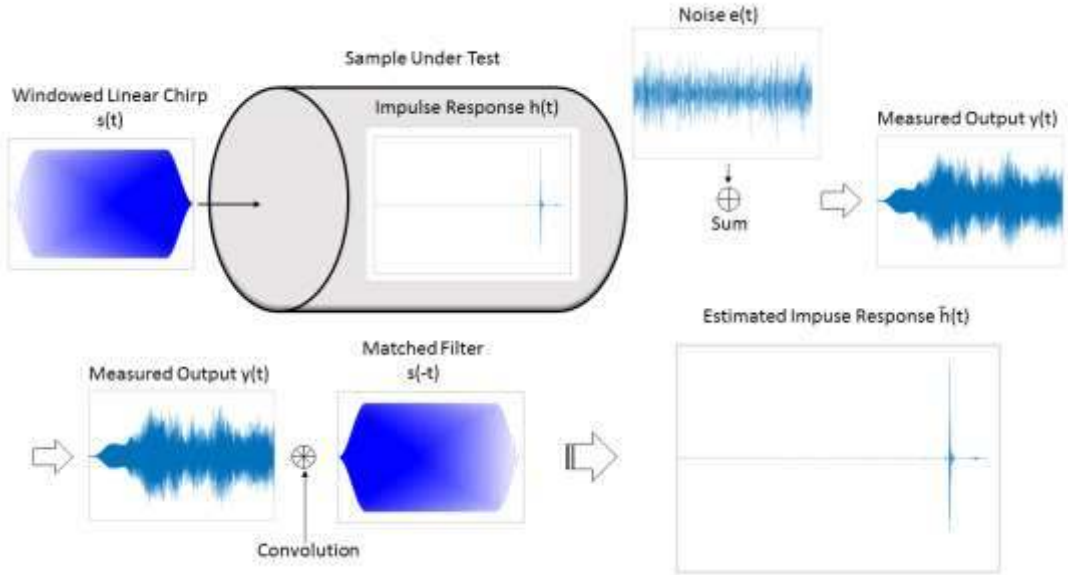

Figure 1. Block diagram of the PuC measurement procedure implemented. A windowed linear chirp is used as coded excitation signal. The output signal, at which is added an Arbitrary White Gaussian Noise, is then filtered with the matched filter, corresponding in the present case to the time reversed replica of the input signal. After the application of the PuC, an estimate of the impulse response, i.e. the reflectogram, is retrieved.

3. Multifrequency AVG analysis

As said, the standard procedure for forgings inspection relies on two pillars: the PuE method and the AVG diagrams. In the previous Section a measurement procedure based

on PuC and alternative to PuE has been introduced to increase the SNR of the measurement and hence the sensitivity of the inspection. In this Section we show how to apply AVG analysis in combination with PuC and how to implement a multi-frequency AVG analysis that can be beneficial when: (1) the optimal inspection frequency is not known; (2) the effect of the inspection frequency on the defect sizing must be considered and (3) an accuracy analysis of the defect sizing capability is of interest.

To accomplish these aims, first of all it is worth to note that, after the application of the PuC procedure, the signals $\hat{h}(t)$ are very similar to those provided by PuE, i.e. $\tilde{h}(t)$, so the standard AVG analysis can be applied on $\hat{h}(t)$ provided that: (i) the AVG diagrams for the Tx-Rx configuration are knows; (ii) the overall measuring system composed by the linear chirp excitation signal and the Tx-Rx probes exhibits a narrowband nature, centred around the frequency f_c of the AVG diagrams one want to use and with relative bandwidth $B_{\%} = \frac{f_2 - f_1}{f_c} \sim 40\%$.

Regarding the point (i), a numerical tool has been implemented that calculate the AVG diagrams by exploiting the Rayleigh-Sommerfeld Integral Model. The two probes have been modelled both as piston transducers and full interference in the path Tx-defect-Rx has been taken into account [13-15]. Regarding the point (ii), usually the narrowband characteristic of the measurement system is guaranteed utilizing narrowband transducers. This is because by using single pulse or short burst excitation the control over the excitation power spectrum is few. Conversely, by employing the PuC with LC signal allows the excitation bandwidth to be shaped with great accuracy and almost arbitrarily, as long as the so-called time-bandwidth product of the chirp $\mathrm{T} \cdot \mathrm{B}$ is large enough, and this is the usual case for forgings inspection. So, the transducers can be also broadband, $B_{\%} > 100$, but the ultrasonic generated spectrum is determined by the chirp. Indeed, when in following Section we consider standard single-frequency analysis, we refer to the use of a narrowband signals, $B_{\%} = 40\%$, that excite broadband transducers (VIDEOSCAN Tx-Rx- pairs from Olympus).

At the same time, the chirp can be designed so that all the transducer bandwidth is uniformly excited. This is generally good in terms of defect detection since a higher bandwidth leads to a higher SNR increment after PuC, but is in conflict with (i).

We therefore investigated if the AVG analysis could be extended to the use of broadband signals and transducers. In this paper we propose and test the following procedure:

1. A broadband LC and a broadband Tx-Rx transducers pair are used;
2. The PuC output $\hat{h}(t)$ undergoes to a bank of digital filters that produce the set of narrowband signals $\{\hat{h}_{f_j}(t)\}$, centred at f_j with $B_{\%} \sim 40$;
3. For each frequency f_j, the standard AVG analysis is applied (the physical attenuation is calculated and counterbalanced numerically, the echo envelope is compared with the AVG diagrams).

An example of the procedure is depicted in Figure 2 while in the following Section some results obtained with both narrowband and broadband chirps are reported.

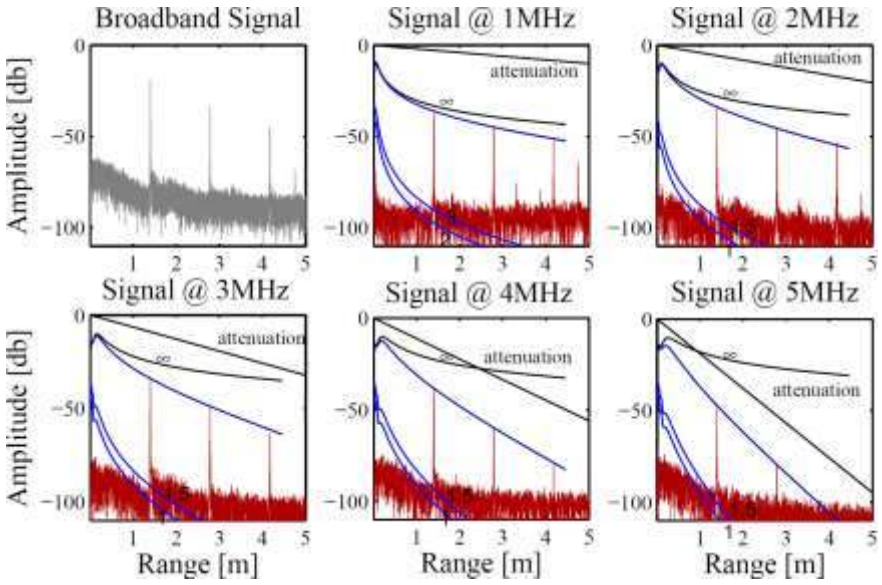

Figure 2. Example of application of the multi-frequency AVG analysis to data collected with broadband probes centred at 5Mhz (Olympus V108 Videoscan). The broadband signal passes to several narrowband filters and the outputs of these filters undergo to a standard single-frequency AVG analysis. The defect detection capability depends on the frequency of the analysis and in this case it is maximum at 3 MHz

In perspective, this method could be further developed to consider only a unique broadband AVG diagram that, by considering the spectrum of the input signal and the frequency-dependent attenuation within the sample, can provide the estimation of the defects size as well as the defect detection sensitivity by exploiting the SNR values and the range resolution of broadband data. It is worth to note that a similar approach has been already considered in calculating standard narrowband AVG to deal with the real bandwidth of the transducers [15].

4. Experimental results

To test both the single-frequency and the multi-frequency AVG analysis, experimental data were collected on a flat bottom hole defect with diameter d=3mm and realized on the back flat surface of a cylindrical forging of diameter ~600 mm and length ~ 1450mm.

Two different pairs of probes were used: a pair of fingertips V109 VIDEOSCAN probes ($\frac{1}{2}$" $active\ element\ diameter$, @5MHz, with centre-centre distance of 17mm) and a pair of V108 VIDEOSCAN probes ($\frac{3}{4}$" $active\ element\ diameter$, @5MHz, with centre-centre distance of 35 mm), both from Olympus. For both Tx-Rx pair, the AVG diagrams were calculated for various central frequencies by means of the numerical simulation tool developed. Figures 3-6 report the results of these analyses.

For single-frequency analysis, the results have been obtained by using narrowband chirp and by repeating the measurement several times by changing the central frequency. For multi-frequency analysis instead the analysis have been carried out by acquiring a single broadband signal and then applying narrowband digital filters before the various AVG analysis It can be seen that the results obtained by using multi-frequency AVG are almost identical to those retrieved by standard AVG

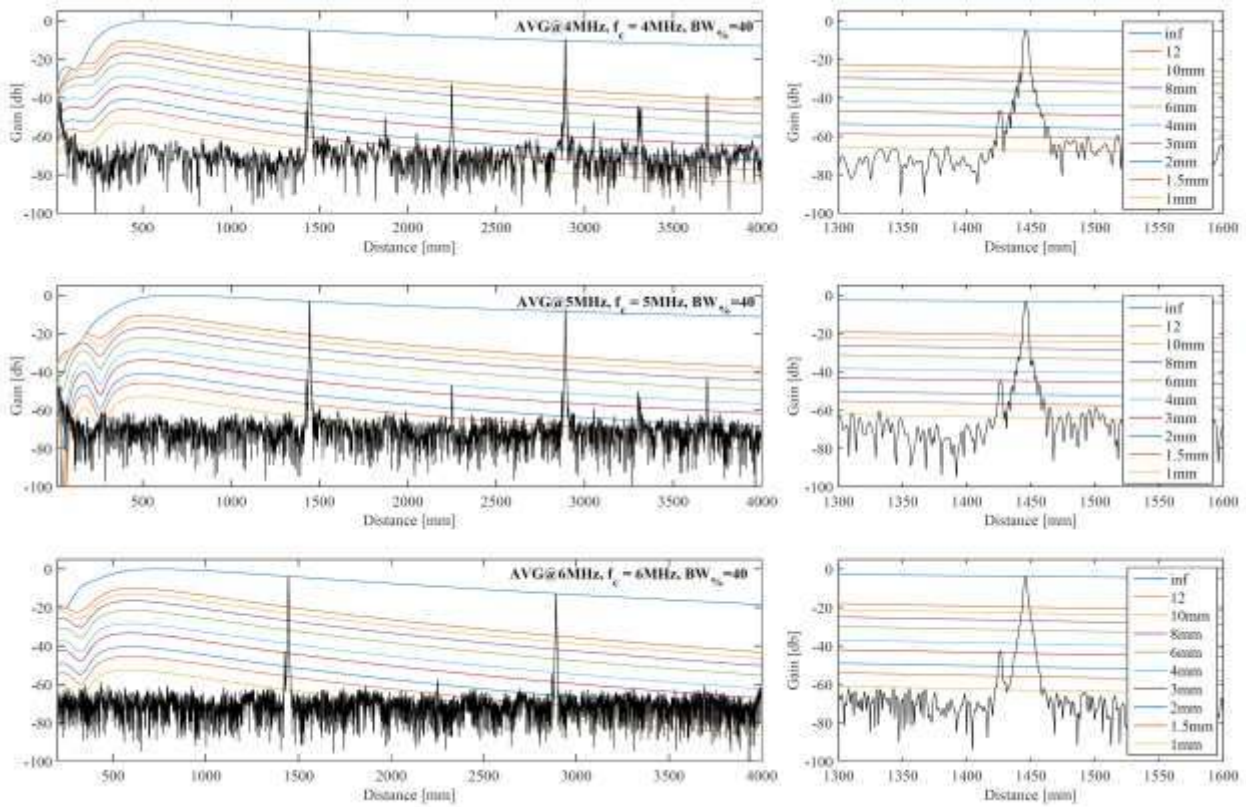

Figure 3. V108 Probes, 3mm diameter flat bottom hole defect: results of single-frequency AVG analysis calculated at different frequencies and by using narrowband linear chirp signals centred at 4,5 and 6 MHz respectively from the top to the bottom.

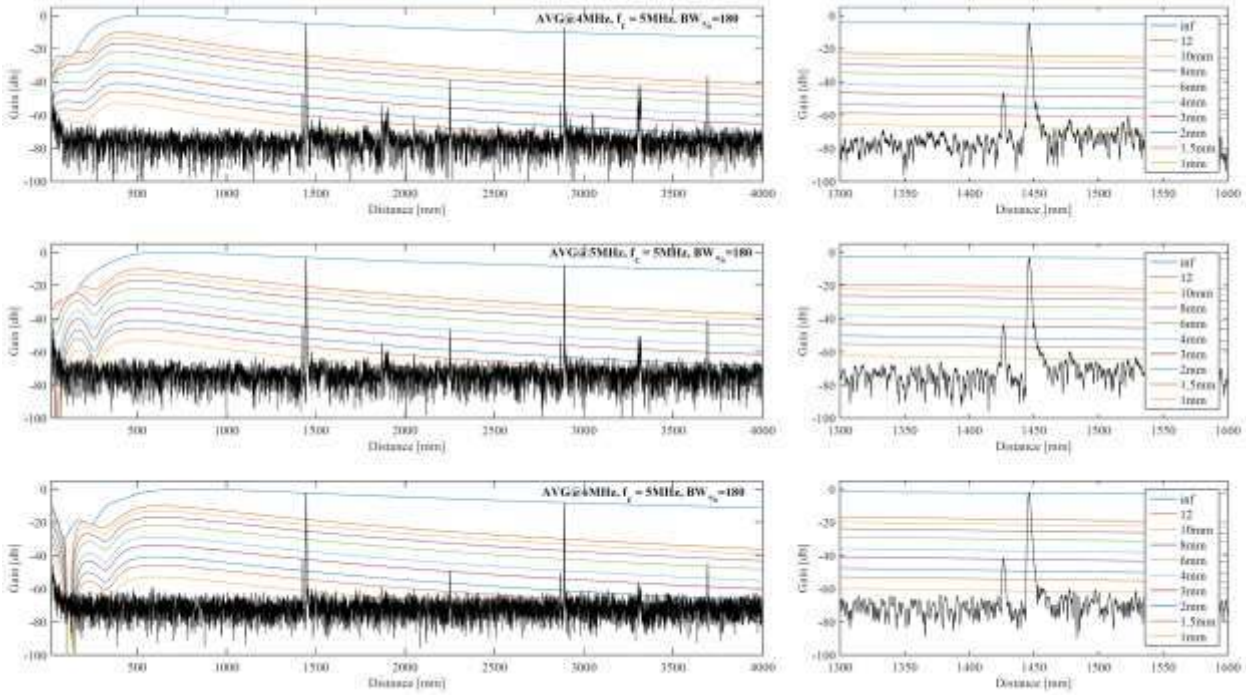

Figure 4. V108 Probes, 3mm diameter flat bottom hole defect: results of multi-frequency AVG analysis calculated at the same frequencies of Figure 3 but using a unique broadband chirp as excitation.

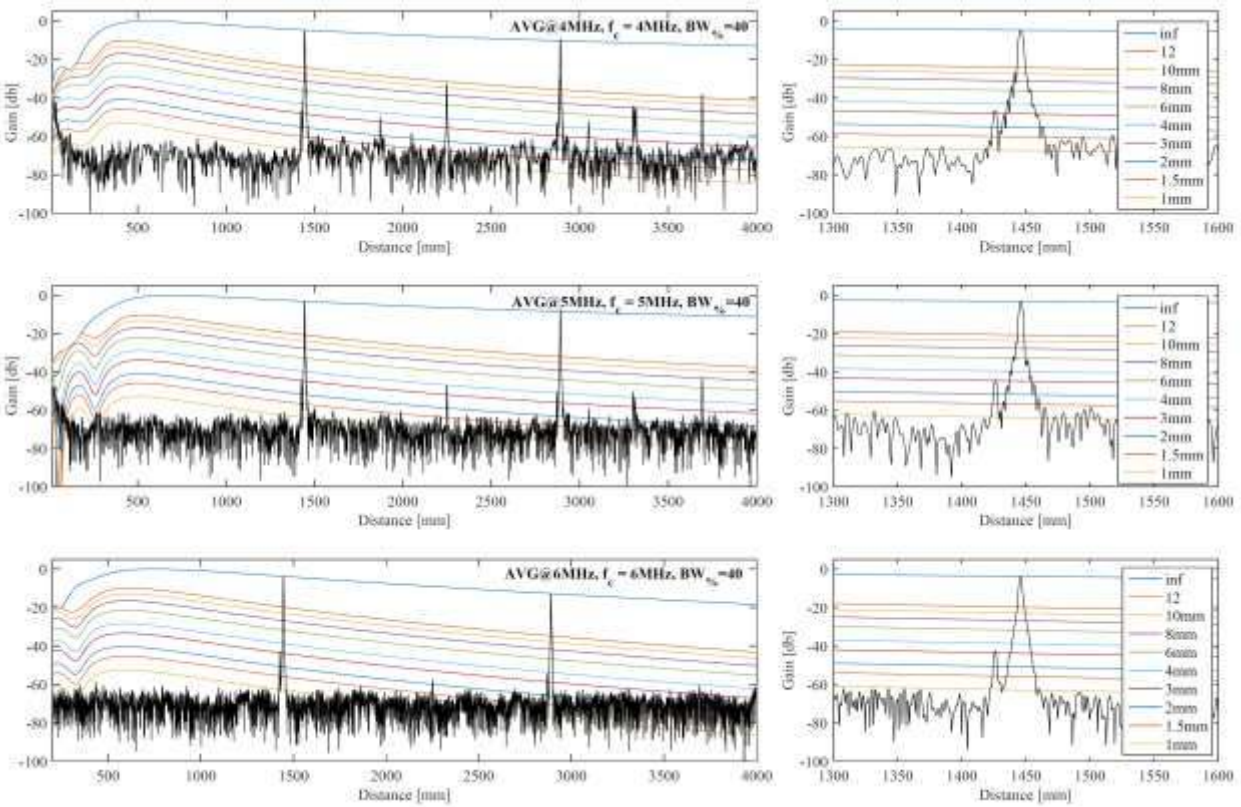

Figure 5. V109 Probes, 3mm diameter flat bottom hole defect: results of single-frequency AVG analysis calculated at different frequencies and by using narrowband linear chirp signals centred at 4,5 and 6 MHz respectively from the top to the bottom.

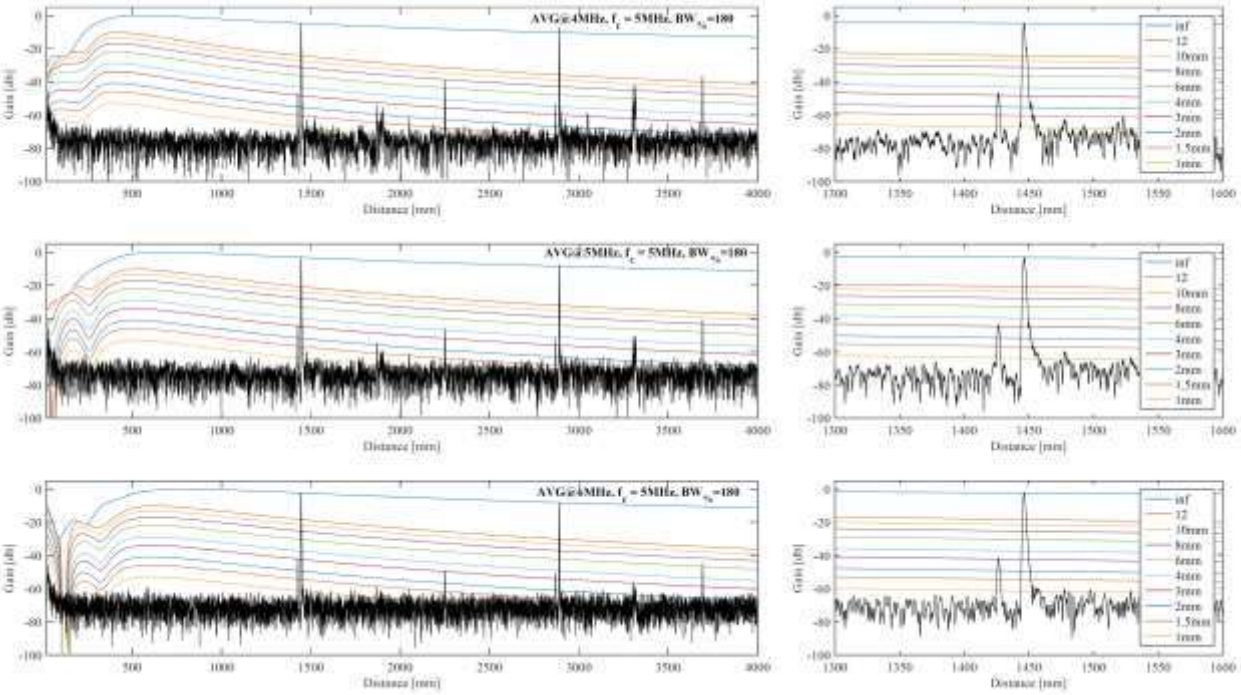

Figure 6. V109 Probes, 3mm diameter flat bottom hole defect: results of multi-frequency AVG analysis calculated at the same frequencies of Figure 4 but using a unique broadband chirp as excitation.

5. Conclusions

An application of the pulse-compression technique to the ultrasonic inspection of forgings is presented. By using broadband probes and broadband excitation, the standard AVG analysis of echograms is extended to contemplate a multi-frequency AVG analysis that allows to individuate the optimal inspection frequency for a given sample. The comparison between broadband and narrowband pulse compression measurements shows that the defect sizing capability is not altered by using broadband signals and transducer and then applying filters before AVG analysis. This results opens the space for further developments for both the optimization of the inspection frequency, and for the development of a broadband AVG defect estimation procedure that could take maximum advantage from PuC in term of SNR gain.

Acknowledgements

This project has received funding from the European Union's Horizon 2020 research and innovation programme under the Marie Skłodowska-Curie grant agreement No 722134 - NDTonAIR". The authors thanks Massimo Calderini, Stefano Neri with Acciai Speciali Terni s.p.a, Renato Borgna, and Matthias Goldammer and Hubert Mooshofer with SIEMENS AG.

References

1. J. Krautkramer., Determination of the size of defects by the ultrasonic impulse echo method. British Journal of Applied Physics. 10, 240-245, 1959.
2. H. Krautkrämer "Detection and Classification of Defects", Ultrasonic Testing of Material, 4th Edition, p. 313-319, (1990).
3. Distance Gain Sizing Technique, European Standard DIN EN583-2:2001
4. Ricci, M., L. Senni, P. Burrascano, R. Borgna, S. Neri, and M. Calderini. "Pulse-compression ultrasonic technique for the inspection of forged steel with high attenuation." Insight-Non-Destructive Testing and Condition Monitoring 54, no. 2 91-95, 2012.
5. G.L. Turin, "An introduction to matched filters," Information Theory, IRE Transactions on , vol.6, no.3, pp.311,329, 1960.
6. T. Misaridis, and J. A. Jensen. "Use of modulated excitation signals in medical ultrasound. Part I: Basic concepts and expected benefits." Ultrasonics, Ferroelectrics, and Frequency Control, IEEE Transactions on 52, no. 2, 177-191, 2005.
7. P. Burrascano, S. Callegari, A. Montisci, M. Ricci, and M. Versaci, eds. Ultrasonic Nondestructive Evaluation Systems: Industrial Application Issues. Springer, 2014.
8. D. Hutchins, P. Burrascano, L. Davis, S. Laureti, and M. Ricci. "Coded waveforms for optimised air-coupled ultrasonic nondestructive evaluation." Ultrasonics 54, no. 7, 1745-1759, 2014.
9. M. Pollakowski, and H. Ermert. "Chirp signal matching and signal power optimization in pulse-echo mode ultrasonic nondestructive testing."Ultrasonics, Ferroelectrics, and Frequency Control, IEEE Transactions on 41, no. 5, 655-659, 1994.

10. P. Pallav, T. H. Gan, and D. Hutchins. "Elliptical-Tukey chirp signal for high-resolution, air-coupled ultrasonic imaging." Ultrasonics, Ferroelectrics, and Frequency Control, IEEE Transactions on 54, no. 8, 1530-1540, 2007.
11. R. E. Challis, and V. G. Ivchenko. "Sub-threshold sampling in a correlation-based ultrasonic spectrometer." Measurement Science and Technology 22, no. 2 (2011): 025902.
12. M. Ricci, L. Senni, P. Burrascano. "Exploiting pseudorandom sequences to enhance noise immunity for air-coupled ultrasonic nondestructive testing." Instrumentation and Measurement, IEEE Transactions on 61, no. 11 (2012): 2905-2915.
13. Schmerr, Lester, and Jung-Sin Song. "Ultrasonic nondestructive evaluation systems". Springer Science+ Business Media, LLC, 2007.
14. Certo, M., G. Nardoni, P. Nardoni, M. Feroldi, and D. Nardoni. "DGS curve evaluation applied to ultrasonic phased array testing." Insight-Non-Destructive Testing and Condition Monitoring 52, no. 4 (2010): 192-194
15. Kleinert, Wolf. Defect Sizing Using Non-destructive Ultrasonic Testing: Applying Bandwidth-dependent Dac and Dgs Curves. Springer, 2016.